Reduced basis methods for Stokes equations in domains with non-affine parameter dependence

Article *in* Computing and Visualization in Science · November 2009

DOI: 10.1007/s00791-006-0044-7 · Source: OAI

1 author:

Gianluigi Rozza
Scuola Internazionale Superiore di Studi Avanzati di Trieste
172 PUBLICATIONS **4,234** CITATIONS

Comput Visual Sci (2009) 12:23–35
DOI 10.1007/s00791-006-0044-7

REGULAR ARTICLE

Reduced basis methods for Stokes equations in domains with non-affine parameter dependence

Gianluigi Rozza

Received: 9 May 2005 / Accepted: 11 July 2006 / Published online: 10 November 2006

Abstract In this paper we deal with reduced basis techniques applied to Stokes equations. We consider domains with different shape, parametrized by affine and non-affine maps with respect to a reference domain. The proposed method is ideally suited for the repeated and rapid evaluations required in the context of parameter estimation, design, optimization, and real-time control. An "empirical", stable and inexpensive interpolation procedure has permitted to replace non-affine coefficient functions with an expansion which leads to a computational decomposition between the off-line (parameter independent) stage for reduced basis generation and the on-line (parameter dependent) approximation stage based on Galerkin projection, used to find a new solution for a new set of parameters by a combination of previously computed stored solutions. As in the affine case this computational decomposition leads us to preserve reduced basis properties: rapid and accurate convergence and computational economies. The applications and results are based on parametrized geometries describing domains with curved walls, for example a stenosed channel and a bypass configuration. This method is well suited to treat also problems in fixed domain with non-affine parameters dependence expressing varying physical coefficients.

Communicated by G. Wittum.

G. Rozza (✉)
Modelling and Scientific Computing (CMCS),
Institute of Analysis and Scientific Computing (IACS),
EPFL, École Polytechnique Fédérale de Lausanne, Station 8,
1015 Lausanne, Switzerland
e-mail: gianluigi.rozza@epfl.ch

1 Introduction to reduced basis framework for viscous flows

The optimization, control, design and characterization of an engineering component or system requires the prediction of certain "quantities of interest", which we denote *outputs* – for example velocity field, maximum stresses, maximum temperatures, heat transfer, flow rates, vorticity, or lifts and drags. These outputs are typically expressed as functionals of field variables associated with parametrized partial differential equations (P^2DE) which describe the system. The parameters, which we shall denote *inputs*, serve to identify a particular "configuration" of the system and may represent design or decision variables, such as geometry, or characterization variables, such as physical properties – for example in inverse design problems. We thus get an implicit *input–output* relationship which demands the solution of the underlying partial differential equations. The approach used to solve P^2DE is based on the reduced-basis methods, first introduced in the late 1970s for non-linear structural analysis (see [2,16]), and later developed more broadly in the 1980s and 1990s (see [3,5] for general framework, [28] for extension to multi-parameter problems, [6,20] for application to non-linear problems). Recent applications of the method on P^2DE are reported in [17,22–24,29,37]. Other works dealing with reduced basis methods applied to incompressible viscous flows are [12,19,35,36], including also control problems as [11]. The reduced-basis methods recognize that the approximate solution is not an arbitrary member of the infinite-dimensional solution space associated with the partial differential equation but it resides on a much lower-dimensional subspace induced by the parametric dependence. More precisely, the reduced basis

methods make use of *global* approximation spaces made up of the (discrete) solutions of P^{2}DE, corresponding to a specific choice of the parameters values. Moreover the computational decomposition between the off-line – parameters independent – stage for reduced basis generation and the on-line – parameters dependent – approximation stage based on Galerkin projection, used to find the solution for a new set of parameters by a combination of previously computed and stored solutions, allows computational economies of several orders of magnitude (see [3] for application of this strategy within the reduced-basis context) or the general a priori convergence theory with respect to the dimension of the reduced basis subspace see, for example, [14,15]. In this paper we deal with the application of reduced basis techniques for Stokes equations in curved parametrized domains. A previous application with affine parameters dependence is presented in [32]. For details dealing with pressure treatment, approximation (LBB equivalent inf-sup condition) and algebraic stability (condition number reduction and basis orthogonalization) in reduced basis Stokes problem we refer to [30]. After this introduction, in Sect. 2 the empirical interpolation procedure proposed in [4] and applied to non-affine transformation terms, mapping the real domain into a reference one is briefly described. The original elements of this work are the use of this interpolation procedure for geometrical non-affine transformation terms, the coupling with the affine ones and the introduction of parametrized complex geometries in the reduced basis problems. In Sect. 3 we present the parametrized Stokes equations framework coupling affine and non-affine parameters dependence. In Sect. 4 we introduce Stokes reduced basis formulation and we recall very briefly approximation stability issue. Then in Sect. 5 we introduce some numerical results based on two different geometries. Finally, in Sect. 6 we give a preview on possible developments for viscous flow and shape optimization [18] problems applied, for example, to haemodynamics [25] within the reduced-basis framework.

2 Empirical interpolation for (coefficient) functions approximation

To start with we recall the empirical interpolation procedure, proposed in [4]. We consider a (coefficient) function $g(x,\mu)$, depending on spatial coordinates and on a set of parameters $\mu \in \mathcal{D} \subset \mathbb{R}^P$ (for some $P \geq 1$). The function $g(x,\mu)$ represents, for example, a coefficient for a linear or bilinear form, that shows up when a non-affine mapping transformation of a physical domain into a reference one indicated with Ω is applied. We assume that $g(x,\mu) \in L^\infty(\Omega)$ for all choice of μ. Our goal is to rewrite this function as an expansion given by products between parameters dependent coefficients and "shape functions" depending only on spacial coordinates so that we may obtain an approximation of $g(x,\mu)$ where both variables are separated. We introduce Ξ^g as a suitably fine parameter sample over $\mathcal{D}$ and the related quantities:

$$\mu_M^g = \arg\max_{\mu\in\Xi^g} \inf_{z\in W_{M-1}^g} \|g(\cdot,\mu) - z\|_{L^\infty(\Omega)}$$

to build the sets $S_M^g = \{\mu_m^g, 1 \leq m \leq M\}, 1 \leq M \leq M_{\max}$, $S_M^g = S_{M-1}^g \cup \mu_M^g$ and the following approximation spaces:

$$W_M^g = \text{span}\{\gamma_m = g(.,\mu_m^g), 1 \leq m \leq M\}, \quad 1 \leq M \leq M_{\max}.$$

The quantity μ_1^g is chosen "a priori" so that $\gamma_1(x) \neq 0$. We need to construct nested sets of interpolation points:

$$\mathcal{T}_M = \{t_1, \ldots t_M\}, \quad 1 \leq M \leq M_{\max}$$

by the following algorithm. Starting from $M = 1$ we store

$$\gamma_1(x) = g\left(x, \mu_1^g\right), \quad t_1 = \arg\sup_{x\in\Omega} |\gamma_1(x)|,$$

$$q_1(x) = \gamma_1(x)/\gamma_1(t_1),$$

for $M \geq 2$ we have to solve a linear system to get σ_{M-1} and then $r_M(x)$ in assembling $\mathcal{T}_M$: $M = 2, \ldots, M_{\max}$:

$$\sum_{j=1}^{M-1} \sigma_j^{M-1} q_j(t_i) = \gamma_M(t_i), \quad 1 \leq i \leq M-1,$$

$$r_M(x) = \gamma_M(x) - \sum_{j=1}^{M-1} \sigma_j^{M-1} q_j(x),$$
$$t_M = \arg\sup_{x\in\Omega} |r_M(x)|,$$
$$q_M(x) = r_M(x)/r_M(t_M).$$

At the end of the algorithm our function is approximated by $g_M(x,\mu)$ and split into two parts (decoupled) each of them depending only on the μ parameter ($\lambda_m(\mu)$) or on x coordinates ($q_m(x)$), i.e.:

$$g_M(x,\mu) = \sum_{m=1}^{M} \lambda_m(\mu) q_m(x),$$

where λ_j are given by the solution of the following linear system:

$$\sum_{j=1}^{M} q_j(t_i)\lambda_j(\mu) = g(t_i,\mu), \quad 1 \leq i \leq M.$$

We choose $M_{\max}$ as being the minimum M s.t. the maximum interpolation error:

$$\varepsilon_M(\mu) = \|g(\cdot,\mu) - g_M(.,\mu)\|_{L^\infty(\Omega)} \tag{1}$$

satisfies $\varepsilon_M \leq \varepsilon_{\max}$ (for a prescribed tolerance $\varepsilon_{\max}$). In computation we restrict by checking (1) in the mesh nodes. The value of μ used is the one of interest we consider each time to calculate our approximated solution. The problem of locally non-affine dependence of $g(x,\mu)$ on parameter μ is also studied in [33].

3 The parametrized Stokes problem

We consider Stokes equations in a domain $\hat{\Omega} \in \mathbb{R}^2$ whose shape is depending on a set of geometrical parameters:

$$\begin{cases} -\nu\triangle\tilde{\mathbf{u}} + \nabla\hat{p} = \hat{\mathbf{f}} & \text{in } \hat{\Omega}, \\ \nabla\cdot\tilde{\mathbf{u}} = 0 & \text{in } \hat{\Omega}, \\ \tilde{\mathbf{u}} = \hat{\mathbf{g}} & \text{on } \Gamma_D, \\ \left(\nu\frac{\partial\tilde{\mathbf{u}}}{\partial\mathbf{n}} - \hat{p}\mathbf{n}\right) = \mathbf{0} & \text{on } \Gamma_N \end{cases} \tag{2}$$

for some given $\hat{\mathbf{f}}$ and $\hat{\mathbf{g}}$. Here Γ_D and Γ_N realize a partition of the boundary Γ of $\hat{\Omega}$. We introduce a lift function $L\hat{\mathbf{g}}$ such that $L\hat{\mathbf{g}} \in (H^1(\hat{\Omega}))^2$ and $L\hat{\mathbf{g}}|_{\Gamma_D} = \hat{\mathbf{g}}$. We denote $\hat{\mathbf{u}} = \tilde{\mathbf{u}} - L\hat{\mathbf{g}}$, where $L\hat{\mathbf{g}}$ here is the continuation in the domain of the boundary condition, so that $\nabla\hat{\mathbf{u}} = \nabla\tilde{\mathbf{u}} - \nabla L\hat{\mathbf{g}}$ and $\hat{\mathbf{u}}|_{\Gamma_D} = \mathbf{0}$. The problem (2) in weak formulation and after the previous assumptions reads: find $\hat{\mathbf{u}} \in \hat{Y} = H^1_{\Gamma_D}(\hat{\Omega}) \times H^1_{\Gamma_D}(\hat{\Omega})$, $\hat{p} \in \hat{Q} = L^2(\hat{\Omega})$, $\hat{\Omega} \subset \mathbb{R}^2$:

$$\begin{cases} \nu\displaystyle\int_{\hat{\Omega}} \nabla\hat{\mathbf{u}}\cdot\nabla\hat{\mathbf{w}}\,\mathrm{d}\hat{\Omega} - \int_{\hat{\Omega}} \hat{p}\nabla\cdot\hat{\mathbf{w}}\,\mathrm{d}\hat{\Omega} \\ = \displaystyle\int_{\hat{\Omega}} \hat{\mathbf{f}}\cdot\hat{\mathbf{w}}\,\mathrm{d}\hat{\Omega} - \nu\int_{\hat{\Omega}} \nabla\hat{\mathbf{g}}\cdot\nabla\hat{\mathbf{w}}\,\mathrm{d}\hat{\Omega}, \quad \forall\,\hat{\mathbf{w}} \in \hat{Y}, \\ \displaystyle\int_{\hat{\Omega}} \hat{q}\,\nabla\cdot\hat{\mathbf{u}}\,\mathrm{d}\hat{\Omega} = -\int_{\hat{\Omega}} \hat{q}\,\nabla\cdot\hat{\mathbf{g}}\,\mathrm{d}\hat{\Omega}, \quad \forall\,\hat{q} \in \hat{Q}, \end{cases} \tag{3}$$

where $H^1_{\Gamma_D}(\hat{\Omega}) = \{v \in (H^1(\Omega)) : v|_{\Gamma_D} = 0\}$. For more details on Stokes problem see, for example, [7,13]. We suppose that the domain is made up of R subdomains: $\hat{\Omega} = \bigcup_{r=1}^R \hat{\Omega}^r$, so that we rewrite (3) as follows:

$$\begin{cases} \langle\hat{\mathcal{A}}\hat{\mathbf{u}},\hat{\mathbf{w}}\rangle + \langle\hat{\mathcal{B}}\hat{p},\hat{\mathbf{w}}\rangle = \langle\hat{F},\hat{\mathbf{w}}\rangle, \quad \forall\,\hat{\mathbf{w}} \in \hat{Y}, \\ -\langle\hat{\mathcal{B}}\hat{q},\hat{\mathbf{u}}\rangle = \langle\hat{G}^0,\hat{q}\rangle, \quad \forall\,\hat{q} \in \hat{Q}, \end{cases} \tag{4}$$

where for $1 \leq i,j \leq d = 2$ and $\hat{\nu}_{i,j} = \nu\delta_{i,j}$,

$$\langle\hat{\mathcal{A}}\hat{\mathbf{u}},\hat{\mathbf{w}}\rangle = \sum_{r=1}^R \int_{\hat{\Omega}^r} \frac{\partial\hat{\mathbf{u}}}{\partial\hat{x}_i}\hat{\nu}_{ij}\frac{\partial\hat{\mathbf{w}}}{\partial\hat{x}_j}\mathrm{d}\hat{\Omega},$$

$$\langle\hat{\mathcal{B}}\hat{p},\hat{\mathbf{w}}\rangle = -\sum_{r=1}^R \int_{\hat{\Omega}^r} \hat{p}\nabla\cdot\hat{\mathbf{w}}\mathrm{d}\hat{\Omega},$$

$$\langle\hat{F},\hat{\mathbf{w}}\rangle = \langle\hat{F}_s,\hat{\mathbf{w}}\rangle + \langle\hat{F}^0,\hat{\mathbf{w}}\rangle.$$

The force field term and the ones due to possible Dirichlet non-homogeneous boundary conditions are given, respectively, by

$$\langle\hat{F}_s,\hat{\mathbf{w}}\rangle = \sum_{r=1}^R \int_{\hat{\Omega}^r} \hat{\mathbf{f}}\hat{\mathbf{w}}\,\mathrm{d}\hat{\Omega}, \quad \langle\hat{F}^0,\hat{\mathbf{w}}\rangle = -\langle\hat{\mathcal{A}}\hat{\mathbf{g}},\hat{\mathbf{w}}\rangle,$$

$$\langle\hat{G}^0,\hat{q}\rangle = \langle\hat{\mathcal{B}}\hat{q},\hat{\mathbf{g}}\rangle.$$

We want to build a system of P^{2}DEs depending on a set of geometrical parameters (μ) as coefficients. Problem (4) is traced back to a *reference domain* by an *affine mapping* on some subdomains $\hat{\Omega}^r_G$ into Ω^r_G and by a *non-affine mapping* on the remaining subdomains $\hat{\Omega}^r_T$ into Ω^r_T . For any $\hat{x} \in \hat{\Omega}^r_G$, $r = 1,\ldots,R_G$, its image $x \in \Omega^r_G$ is given by

$$x = G^r(\mu)\hat{x} + g^r, \quad 1 \leq r \leq R_G,$$

where g^r is not depending on spatial coordinates. We thus write on Ω^r_G

$$\frac{\partial}{\partial\hat{x}_i} = \frac{\partial x_j}{\partial\hat{x}_i}\frac{\partial}{\partial x_j} = G^r_{ji}(\mu)\frac{\partial}{\partial x_j}.$$

For any $\hat{x} \in \hat{\Omega}^r_T$, $r = 1,\ldots,R_T$, its image $x \in \Omega^r_T$ is given by

$$x = T^r(\mu,\hat{x}) + \kappa^r, \quad 1 \leq r \leq R_T,$$

where also κ^r does not depend on x. We thus write on Ω^r_T

$$\frac{\partial}{\partial\hat{x}_i} = \frac{\partial x_j}{\partial\hat{x}_i}\frac{\partial}{\partial x_j} = T^r_{ji}(\mu,x)\frac{\partial}{\partial x_j};$$

we recall that $R = R_G + R_T$ and $\Omega = \sum_{r=1}^{R_G}\Omega^r_G + \sum_{r=1}^{R_T}\Omega^r_T$. In the reference domain Ω we have

$$\langle\mathcal{A}\mathbf{u},\mathbf{w}\rangle = \sum_{r=1}^{R_G}\int_{\Omega^r_G} \frac{\partial\mathbf{u}}{\partial x_i}\nu^r_{G_{ij}}(\mu)\frac{\partial\mathbf{w}}{\partial x_j}\mathrm{d}\Omega + \sum_{r=1}^{R_T}\int_{\Omega^r_T} \frac{\partial\mathbf{u}}{\partial x_i}\nu^r_{T_{ij}}(\mu,x)\frac{\partial\mathbf{w}}{\partial x_j}\mathrm{d}\Omega, \quad \forall\,\mathbf{w} \in Y,$$

$$\langle \mathcal{B}p, \mathbf{w}\rangle = -\sum_{r=1}^{R_G} \int_{\Omega_G^r} p\chi_{G_{ij}}^r(\mu)\frac{\partial w_j}{\partial x_i}\mathrm{d}\Omega - \sum_{r=1}^{R_T} \int_{\Omega_T^r} p\chi_{T_{ij}}^r(\mu,x)\frac{\partial w_j}{\partial x_i}\mathrm{d}\Omega, \quad \forall \mathbf{w}\in Y,$$

$$\langle F, \mathbf{w}\rangle = \langle F_s, \mathbf{w}\rangle + \langle F^0, \mathbf{w}\rangle,$$

where

$$\langle F_s, \mathbf{w}\rangle = \sum_{r=1}^{R_G} \int_{\Omega_G^r} \left(\hat{\mathbf{f}}^r \det(G^r(\mu))^{-1}\right)\mathbf{w}\mathrm{d}\Omega + \sum_{r=1}^{R_T} \int_{\Omega_T^r} \left(\hat{\mathbf{f}}^r \det(T^r(\mu,x))^{-1}\right)\mathbf{w}\mathrm{d}\Omega,$$

$$\langle F^0, \mathbf{w}\rangle = -\langle \mathcal{A}\mathbf{g}, \mathbf{w}\rangle;\ \langle G^0, q\rangle = \langle \mathcal{B}q, \mathbf{g}\rangle.$$

The *transformation tensors* used above for viscous bilinear forms with affine and non-affine mappings are defined, respectively, as follows:

$$\nu_{G_{ij}}^r(\mu) = G_{ii'}^r(\mu)\hat{\nu}_{i'j'}G_{jj'}^r(\mu)\det(G^r(\mu))^{-1},\quad 1\le i,\ j\le 2,\ r=1,\ldots,R_G; \tag{5}$$

$$\nu_{T_{ij}}^r(\mu,x) = T_{ii'}^r(\mu,x)\hat{\nu}_{i'j'}T_{jj'}^r(\mu,x)\det(T^r(\mu,x))^{-1},\quad 1\le i,\ j\le 2,\ r=1,\ldots,R_T. \tag{6}$$

The tensors for *pressure and divergence linear forms* are defined, respectively, for affine and non-affine mappings as

$$\chi_{G_{ij}}^r(\mu) = G_{ij}^r\det(G^r(\mu))^{-1}, \tag{7}$$

$$\chi_{T_{ij}}^r(\mu,x) = T_{ij}^r(\mu,x)\det(T^r(\mu,x))^{-1}. \tag{8}$$

In Sect. 5 we introduce two different parameterization based on different test cases and we show their explicit forms. For the non-affine parts we apply the empirical interpolation procedure of Sect. 2 to expand non-affine mapping terms and decouple the parameters dependent contribution from the one depending only on spacial coordinates. We transform (6) and (8), respectively, in the following formulations:

$$\nu_{T_{ij}}^r(\mu,x) = \sum_{m=1}^{M_{ijr}^a}\beta_{ijm}^r(\mu)\gamma_{ijm}^r(x), \tag{9}$$

$$\chi_{T_{ij}}^r(\mu,x) = \sum_{m=1}^{M_{ijr}^b}\alpha_{ijm}^r(\mu)\omega_{ijm}^r(x), \tag{10}$$

where m refers to the number of interpolation functions we use for each form (related with max interpolation error), i and j are indexes related to linear/bilinear form, r refers to subdomains. β and α are weight quantities depending on the parameters μ, while γ and ω are interpolation functions used as basis.

Furthermore, we may define

$$\Theta^{q(i,j,r)}(\mu) = \nu_{G_{ij}}^r(\mu),\quad \mathcal{A}_G^{q(i,j,r)}(\mathbf{u},\mathbf{w}) = \int_{\Omega_G^r}\frac{\partial \mathbf{u}}{\partial x_i}\frac{\partial \mathbf{w}}{\partial x_j}\mathrm{d}\Omega,$$

$$\Phi^{s(i,j,r)}(\mu) = \chi_{G_{ij}}^r(\mu),\quad \mathcal{B}_G^{s(i,j,r)}(p,\mathbf{w}) = -\int_{\Omega_G^r} p\frac{\partial w_i}{\partial x_j}\mathrm{d}\Omega$$

for $1\le r\le R_G$, $1\le i,j\le d=2$ (q and s are condensed indexes of i,j,r quantities)

$$\Psi^{t(i,j,r,m)}(\mu) = \beta_{ijm}^r(\mu),$$

$$\mathcal{A}_T^{t(i,j,r,m)}(\gamma(x),\mathbf{u},\mathbf{w}) = \int_{\Omega_T^r}\gamma_{ijm}^r(x)\frac{\partial \mathbf{u}}{\partial x_i}\frac{\partial \mathbf{w}}{\partial x_j}\mathrm{d}\Omega,$$

$$\Upsilon^{p(i,j,r,m)}(\mu) = \alpha_{ijm}^r(\mu),$$

$$\mathcal{B}_T^{p(i,j,r,m)}(\omega(x),p,\mathbf{w}) = -\int_{\Omega_T^r}\omega_{ijm}^r(x)p\frac{\partial w_i}{\partial x_j}\mathrm{d}\Omega$$

for $1\le r\le R_T, 1\le i,j\le d=2, 1\le m\le \max(M_{ijr}^a, M_{ijr}^b)$ (t and p are condensed indexes of i,j,r,m quantities). Finally, we may apply an effectively affine decomposition:

$$\mathcal{A}(\mu,\mathbf{u},\mathbf{w}) = \sum_{q=1}^{Q_G^a}\Theta^q(\mu)\mathcal{A}_G^q(\mathbf{u},\mathbf{w}) + \sum_{t=1}^{Q_T^a}\Psi^t(\mu)\mathcal{A}_T^t(\gamma(x),\mathbf{u},\mathbf{w}),$$

$$\mathcal{B}(\mu,p,\mathbf{w}) = \sum_{s=1}^{Q_G^b}\Phi^s(\mu)\mathcal{B}_G^s(p,\mathbf{w}) + \sum_{p=1}^{Q_T^b}\Upsilon^p(\mu)\mathcal{B}_T^p(\omega(x),p,\mathbf{w}).$$

In general $\max(Q_G^a) = d\times d\times d\times R_G, \max(Q_G^b) = d\times d\times R_G$; $Q_T^a = \sum_{j=1}^d\sum_{i=1}^d\sum_{r=1}^{R_T} M_{ijr}^a$; $Q_T^b = \sum_{j=1}^d\sum_{i=1}^d\sum_{r=1}^{R_T} M_{ijr}^b$. The Stokes problem rewritten on the reference domain Ω reads: find $(\mathbf{u}(\mu),p(\mu))\in Y\times Q$

$$\begin{cases}\mathcal{A}(\mu;\mathbf{u}(\mu),\mathbf{w}) + \mathcal{B}(\mu;p(\mu),\mathbf{w}) = \langle F,\mathbf{w}\rangle, & \forall \mathbf{w}\in Y\\ \mathcal{B}(\mu;q,\mathbf{u}(\mu)) = \langle G^0,q\rangle, & \forall q\in Q,\end{cases} \tag{11}$$

where here $Y = H_{\Gamma_D}^1(\Omega)\times H_{\Gamma_D}^1(\Omega)$ and $Q = L^2(\Omega)$. This problem has an inf–sup condition (LBB) [27] to be

guaranteed for the stability:

$$\beta(\mu) = \inf_{q\in Q}\sup_{\mathbf{w}\in Y}\frac{\mathcal{B}(\mu,q,\mathbf{w})}{\|\mathbf{w}\|_Y\|q\|_Q} \geq \beta_0 > 0, \quad \forall\,\mu \in \mathcal{D}.$$

To prove it we introduce a so-called supremizer operator $T^\mu\colon Q \to Y$ so that

$$(T^\mu q,\mathbf{w})_Y = \mathcal{B}(\mu;q,\mathbf{w}), \quad \forall\,\mathbf{w} \in Y. \tag{12}$$

It is readily shown that

$$T^\mu q = \arg\sup_{\mathbf{w}\in Y}\frac{\mathcal{B}(\mu;q,\mathbf{w})}{\|\mathbf{w}\|_Y},$$

then

$$\beta^2(\mu) = \inf_{q\in Q}\frac{(T^\mu q, T^\mu q)_Y}{\|q\|_Q^2}.$$

For the proofs see [30].

The Stokes problem has been solved by Galerkin-Finite Element method using Taylor–Hood $\mathbb{P}^2-\mathbb{P}^1$ elements for velocity and pressure, respectively [34]. See also [8–10].

4 The Stokes reduced basis formulation

In the reduced basis approximation we construct a set of "μ" parameters samples $S_N^\mu = \{\mu^1,\ldots,\mu^N\}$, where $\mu^n \in \mathcal{D}^\mu$, $n = 1,\ldots,N$. Correspondingly, we define a set of couples $(\mathbf{u}_h(\mu^n), p_h(\mu^n))$ which are approximate solutions of the Stokes problem (11) using Galerkin-Finite Element method and computed in the same reference domain. Then the *reduced-basis pressure space* is $Q_N = \text{span}\{\xi_n(n=1,\ldots,N)\}$, where $\xi_n = p_h(\mu^n)$, while the *reduced-basis velocity space* is $Y_N = \text{span}\,\{\zeta_n(n = 1,\ldots,N); T^{\mu^n}\xi_n(n = 1,\ldots,N)\}$, where $\zeta_n = \mathbf{u}_h(\mu^n)$. Supremizer solutions $T^{\mu^n}\xi_n$ are computed solving the problem (12) with finite element method and they enrich velocity reduced basis approximation space.

The problem in reduced basis approximation reads: find $(\mathbf{u}_N(\mu), p_N(\mu)) \in Y_N \times Q_N$ s.t.:

$$\begin{cases} \mathcal{A}(\mu;\mathbf{u}_N(\mu),\mathbf{w}) + \mathcal{B}(\mu;p_N(\mu),\mathbf{w}) = \langle F,\mathbf{w}\rangle, & \forall\,\mathbf{w} \in Y_N \\ \mathcal{B}(\mu;q,\mathbf{u}_N(\mu) = \langle G^0,q\rangle, & \forall\,q \in Q_N. \end{cases} \tag{13}$$

This problem is well posed if it does admit an inf-sup property. We introduce

$$\beta_N(\mu) = \inf_{q\in Q_N}\sup_{\mathbf{w}\in Y_N}\frac{\mathcal{B}(\mu,q,\mathbf{w})}{\|\mathbf{w}\|_Y\|q\|_Q},$$

and it is shown in [30] that thanks to the enrichment of velocity approximation space operated by supremizer solutions the following condition is fulfilled:

$$\beta_N(\mu) \geq \beta_h(\mu) \geq \beta_0 > 0, \quad \forall\,\mu \in \mathcal{D}^\mu,$$

where $\beta_h(\mu)$ is the inf-sup constant related to Galerkin-Finite Element Method. We rewrite for computational convenience Y_N using the *effectively affine dependence* of $\mathcal{B}(\mu;q,\mathbf{w})$ on the parameter and the *linearity* of T^μ:

$$T^\mu\xi = \sum_{q=1}^{Q_G^b}\Phi^q(\mu)T_G^q\xi + \sum_{p=1}^{Q_T^b}\Upsilon^p(\mu)T_T^p\xi, \tag{14}$$

for any ξ and μ, where:

$$(T_G^q\xi,\mathbf{w})_Y = \mathcal{B}_G^q(q,\mathbf{w}), \quad \forall\,\mathbf{w} \in Y,$$
$$(T_T^p\xi,\mathbf{w})_Y = \mathcal{B}_T^p(\omega,q,\mathbf{w}), \quad \forall\,\mathbf{w} \in Y,$$

which allows us to write:

$$Y_N = \text{span}\left\{\sum_{k=1}^{\overline{Q}_G^b}\Phi^k(\mu^n)\sigma_{kn} + \sum_{k'=1}^{Q_T^b}\Upsilon^{k'}(\mu^n)\widetilde{\sigma}_{k'n} \quad (n=1,\ldots,2N)\right\},$$

where $\overline{Q}_G^b = Q_G^b + 1, \Phi^{\overline{Q}_G^b} = 1, \mu^{N+j} = \mu^j, 1 \leq j \leq N$. For $n = 1,\ldots,N$:

$$\sigma_{kn} = 0, \quad \text{for } k = 1,\ldots,Q_G^b;$$
$$\widetilde{\sigma}_{k'n} = 0, \quad \text{for } k' = 1,\ldots,Q_T^b;$$
$$\sigma_{\overline{Q}_G^b n} = \zeta_n = \mathbf{u}(\mu^n).$$

For $n = N+1,\ldots,2N$:

$$(\sigma_{kn},\mathbf{w})_Y = \mathcal{B}_G^k(\xi_{n-N},\mathbf{w}), \quad \forall\,\mathbf{w} \in Y, \text{ for } k = 1,\ldots,Q_G^b;$$
$$\sigma_{\overline{Q}_G^b n} = 0;$$
$$(\widetilde{\sigma}_{kn},\mathbf{w})_Y = \mathcal{B}_T^k(\omega,\xi_{n-N},\mathbf{w}), \quad \forall\,\mathbf{w} \in Y, \text{ for } k = 1,\ldots,Q_T^b.$$

For a new "μ" we want a solution given by a combination of previously computed stored solutions as basis functions:

$$\mathbf{u}_N(\mu) = \sum_{j=1}^{2N}u_{Nj}(\mu)\left(\sum_{k=1}^{\overline{Q}_G^b}\Phi^k(\mu^j)\sigma_{kj} + \sum_{k'=1}^{Q_T^b}\Upsilon^{k'}(\mu^j)\widetilde{\sigma}_{k'j}\right),$$

$$p_N(\mu) = \sum_{l=1}^{N}p_{Nl}(\mu)\xi_l,$$

whose weights $\mathbf{u}_{Nj}$ and p_{Nl} are given by the following reduced basis linear system:

$$\begin{cases} \sum_{j=1}^{2N} A_{ij}^{\mu} u_{Nj}(\mu) + \sum_{l=1}^{N} B_{il}^{\mu} p_{Nl}(\mu) = F_i, \quad 1 \le i \le 2N \\ \sum_{j=1}^{2N} B_{jl}^{\mu} u_{Nj}(\mu) = G_l, \quad 1 \le l \le N \end{cases} \tag{15}$$

where the sub-matrices A and B are given by

$$\begin{aligned} A_{ij}^{\mu} &= \sum_{k=1}^{Q_G^a} \sum_{k'=1}^{\overline{Q}_G^b} \sum_{k''=1}^{\overline{Q}_G^b} \Theta^k(\mu) \Phi^{k'}(\mu^i) \Phi^{k''}(\mu^j) \mathcal{A}_G^k(\sigma_{k'i}, \sigma_{k''j}) \\ &+ \sum_{k=1}^{Q_T^a} \sum_{k'=1}^{Q_T^b} \sum_{k''=1}^{Q_T^b} \Psi^k(\mu) \Upsilon^{k'}(\mu^j) \Upsilon^{k''}(\mu^i) \mathcal{A}_T^k(\gamma, \widetilde{\sigma}_{k'i}, \widetilde{\sigma}_{k''j}), \\ &\quad 1 \le i, \ j \le 2N; \\ B_{il}^{\mu} &= \sum_{k=1}^{Q_G^b} \sum_{k'=1}^{\overline{Q}_G^b} \Phi^k(\mu) \Phi^{k'}(\mu^i) \mathcal{B}_G^k(\sigma_{k'i}, \xi_l) \\ &+ \sum_{k=1}^{Q_T^b} \sum_{k'=1}^{Q_T^b} \Upsilon^k(\mu) \Upsilon^{k'}(\mu^i) \mathcal{B}_T^k(\omega, \widetilde{\sigma}_{k'i}, \xi_l), \\ &\quad 1 \le i \le 2N, \quad 1 \le l \le N; \end{aligned}$$

and:

$$\begin{aligned} F_i &= \sum_{k'=1}^{\overline{Q}_G^b} \Phi^{k'}(\mu^i) \langle F, \sigma_{k'i} \rangle + \sum_{k'=1}^{Q_T^b} \Upsilon^{k'}(\mu^i) \langle F, \widetilde{\sigma}_{k'i} \rangle, \\ &\quad 1 \le i \le 2N, \\ G_l &= \langle G^0, \xi_l \rangle, \quad 1 \le l \le N. \end{aligned}$$

System (15) can therefore be written as

$$\begin{pmatrix} A & B \\ B^{\mathrm{T}} & 0 \end{pmatrix} \cdot \begin{pmatrix} u_N \\ p_N \end{pmatrix} = \begin{pmatrix} F \\ G \end{pmatrix}. \tag{16}$$

Remark 1 Note that more options dealing with the supremizer calculation and basis assembling procedures are available. At this step we have adopted the second alternative option introduced in [30], where all the velocity reduced basis functions are μ (on-line) independent (they depend only on samples μ^j used to store basis). This option grants us in practice the possibility to apply basis orthogonalization (Gram–Schmidt) to achieve algebraic stability (controlling conditioning numbers of reduced basis matrices) satisfying at the same time also approximation stability and inf-sup condition. This option is also competitive concerning computational costs dealing with $3N \times 3N$ reduced basis matrices (16) instead of $(\overline{Q}^b + 1)N \times (\overline{Q}^b + 1)N$ matrix (usually $(\overline{Q}^b + 1) \gg 3$, $\overline{Q}^b = \overline{Q}_G^b + Q_T^b$) introduced as the first option to build reduced basis velocity space in [30] without the use of (14) before applying orthogonalization.

Remark 2 We have the following on-line computational costs to build reduced basis matrices, given also the supremizer components in the velocity space: $O(Q^a 4N^2)$ for sub-matrix A, $O((Q^b)2N^2)$ for B, $O(N)$ for F and $O(9N^3)$ for the inversion of the full reduced basis matrix (16), where $Q^a = Q_T^a + Q_G^a$, $Q^b = Q_G^b + Q_T^b$. Note that the quantities Q_G^a and Q_G^b are depending only on the number of subdomains with affine mappings (R_G), while quantities Q_T^a and Q_T^b are depending also on the number of "shape functions" ($\gamma(x)$ and $\omega(x)$) related with interpolation error ($\varepsilon_{\max}$) and the number of subdomains with non-affine mappings (R_T).

4.1 An adaptive procedure to build reduced basis efficiently

An adaptive procedure based on H^1 max relative error for velocity E_{H^1} has been developed to optimize basis assembling, optionally we can also consider and combine L^2 maximum relative error for pressure E_{L^2}. We underline that, given the higher powers of N that appear in our cost computing estimation, it is crucial (both for on-line and off-line effort) to control N more tightly. We first construct, off-line, an approximation that, over most of the domain, exhibits an error ϵ (E_{H^1} or E_{L^2} or both) less than $\epsilon_d^{\text{prior}}$: we begin with a first sample $\mu^1 (S_{N'=1} = \{\mu^1\})$; we next evaluate error $\epsilon_{N'=1}(\mu)$ over a large test set of parameter samples in $\mathcal{D}^{\mu}$, denoted with Σ^{prior}; we then choose for μ^2 (and hence $S_{N'=2} = \{\mu^1, \mu^2\}$) the maximizer of $\epsilon_{N'=1}(\mu)$ over Σ^{prior}. We repeat this process until the maximum of $\epsilon_{N'=N^{\text{prior}}}(\mu)$ over Σ^{prior} is lower than $\epsilon_d^{\text{prior}}$. Then, on-line, given a new value of the parameter, μ, and an error tolerance $\epsilon_d^{\text{post}}(\mu)$, we essentially repeat this adaptive process – but now our sample points are drawn from $S_{N^{\text{prior}}}$, and the test sample is a singleton – μ. Typically we choose $\epsilon_d^{\text{prior}} \ll \epsilon_d^{\text{post}}(\mu)$ since our test is not exhaustive; and therefore, typically, $N^{\text{post}}(\mu) \ll N^{\text{prior}}$. With the adaptive process we get higher accuracy at lower N: modest reductions in N can translate into measurable performance improvements. This procedure is very important not only to get a computationally cheaper and faster procedure but also to avoid ill-conditioning in matrix assembling procedures. Usually in multi-parameter problems samples

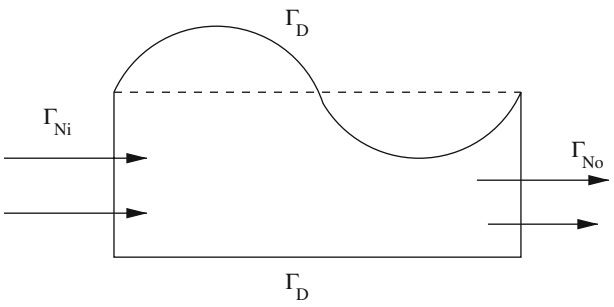

Fig. 1 Geometrical scheme for the stenosis test problem ($\mu = -0.5$)

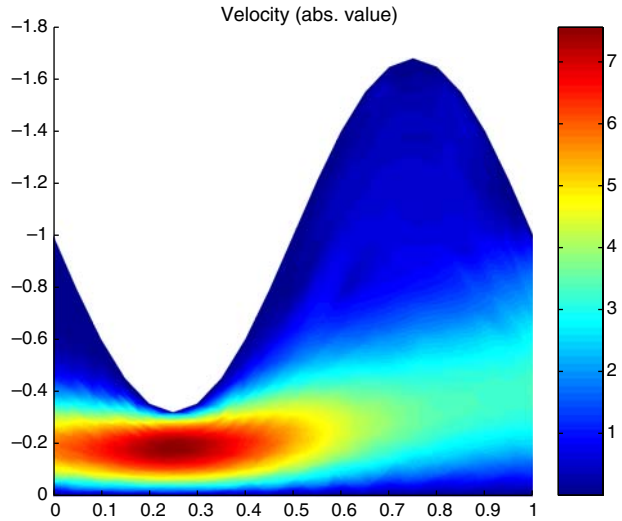

Fig. 2 The stenosis test problem ($\mu = 0.5$): velocity (absolute value) [m s^{-1}]

are properly chosen in their range of variation to cover all the parameters' space (see for example Fig. 7).

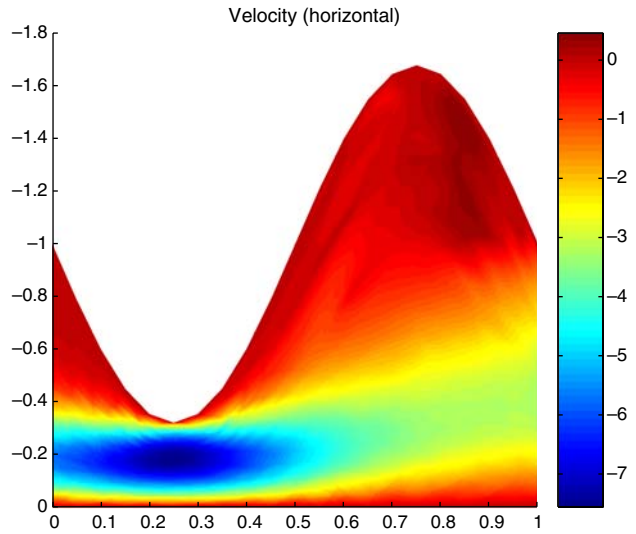

Fig. 3 $\mu = 0.5$: horizontal velocity [m s^{-1}]

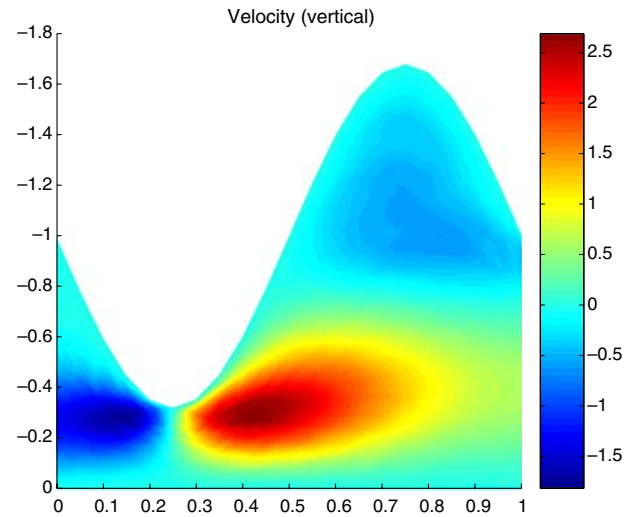

Fig. 4 $\mu = 0.5$: vertical velocity [m s^{-1}]

5 Numerical results

Numerical tests were carried out to develop Stokes reduced basis with affine/non-affine mappings. Taylor–Hood finite elements have been used to store approximation basis functions: $\mathbb{P}^2 - \mathbb{P}^1$ elements for velocity (with supremizer) and pressure, respectively [27].

At this step the reduced basis solutions have been compared directly with approximate finite element solutions by computing the H^1 relative error for velocity and the L^2 relative error for pressure.

5.1 First test: curved upper wall

In this first test we apply empirical interpolation to describe a channel with a curved and parametrized upper wall. This simple geometry (see Fig. 1) can be considered for example in the study of blood flow through an artery occluded by a stenosis, i.e. featuring a reduced section (see [25]). A similar geometry can be used also in periodical series to set up and study an oxigenator for haemodynamic applications. In our application we have made the following assumptions:

– To solve the parametrized Stokes problem in the domain outlined in Fig. 1 we have imposed zero Dirichlet conditions on the boundary Γ_D, Neumann non-homogeneous conditions on the inflow Γ_{Ni} ($\tau_n = 1, \tau_t = 0$, where $\tau = (\nu \frac{\partial \mathbf{u}}{\partial \mathbf{n}} - p\mathbf{n})$, with n and t normal and tangential directions, respectively) and Neumann

homogeneous conditions on outflow Γ_{No} ($\tau_n = 0$, $\tau_t = 0$).

– We consider one parameter μ (range: $[-0.8, 0.8]$) to describe the upper arterial wall in the physical domain, through $\hat{x}_2 = f(\mu, \hat{x}_1) = 1 + \mu \cdot \sin(2\pi \hat{x}_1)$ (we have a single domain subject to an unique non-affine mapping). Referring to Sect. 3 we have $\Omega_G = \emptyset$ and $\Omega_T = \Omega$, so $R_T = 1$. See Fig. 2–4
The coordinate transformation is $T : \hat{\Omega} \to \Omega$ such as $x = T(\hat{x})$ and

$$(x_1, x_2) = T(\hat{x}_1, \hat{x}_2) = \left(\hat{x}_1, \frac{1}{f(\mu, \hat{x}_1)} \hat{x}_2\right) \tag{17}$$

in Ω. Then,

$$\mathrm{d}\hat{x}_1 \mathrm{d}\hat{x}_2 = f(\mu, x_1) \mathrm{d}x_1 \mathrm{d}x_2$$

and the following relations hold:

$$\begin{cases} \frac{\partial \hat{\mathbf{u}}}{\partial \hat{x}_2} = \frac{1}{f(\mu, x_1)} \frac{\partial \mathbf{u}}{\partial x_2}, \\ \frac{\partial \hat{\mathbf{u}}}{\partial \hat{x}_1} = \frac{\partial \mathbf{u}}{\partial x_1} - x_2 \frac{f_{x_1}(\mu, x_1)}{f(\mu, x_1)} \frac{\partial \mathbf{u}}{\partial x_2} \end{cases} \left(\text{with } f_{x_1} := \frac{\mathrm{d}f}{\mathrm{d}x_1}\right), \tag{18}$$

$$\nabla \cdot \hat{\mathbf{u}} = \frac{\partial u_1}{\partial x_1} - x_2 \frac{f_{x_1}(\mu, x_1)}{f(\mu, x_1)} \frac{\partial u_1}{\partial x_2} + \frac{1}{f(\mu, x_1)} \frac{\partial u_2}{\partial x_2}. \tag{19}$$

Using the compact notation of Sect. 3 [(6) and (8)] and transformation (17) we get the following tensor for diffusion and divergence forms, respectively:

$$\nu_T = \nu \begin{bmatrix} f(\mu, x_1) & -f'_{x_1}(\mu, x_1) x_2 \\ -f'_{x_1}(\mu, x_1) x_2 & \frac{1}{f(\mu, x_1)} + \frac{f'^2_{x_1}(\mu, x_1)}{f(\mu, x_1)} x_2{}^2 \end{bmatrix}; \tag{20}$$

$$\chi_T = \begin{bmatrix} f(\mu, x_1) & -f'_{x_1}(\mu, x_1) x_2 \\ 0 & 1 \end{bmatrix}; \tag{21}$$

where $\nu = 0.04\,\mathrm{sm}^{-2}$ is the viscosity. Referring to notation of Sect. 2 we get five different coefficients functions $g^j_M(\mu, x)$ to expand.

– We apply empirical interpolation [(9) and (10)] to the tensors [(20) and (21)] and we impose a maximum interpolation error $\varepsilon_{\max}$, thus considering different $M_{\max}$ "shape functions" for every $g^j_M(\mu, x)$. Each $g^j_M(x, \mu)$ refers to a different coefficient of a bilinear form of our Stokes problem ($j = 5$ in this test case). Owing to empirical interpolation we expand each tensor component to apply the effectively affine decomposition:

Table 1 Mean H^1 velocity relative errors for $\varepsilon_{\max} = 10^{-1}$ and $\varepsilon_{\max} = 10^{-2}$, imposed on all $g^j_M(x, \mu)$ (considering several different μ test values)

N	$\varepsilon_{\max} = 0.1$	$\varepsilon_{\max} = 0.01$
1	2.2549e+000	4.2557e−001
2	2.1926e+000	1.3614e−001
3	2.1361e+000	2.1768e−002
4	2.1267e+000	1.5939e−002
5	2.1226e+000	4.9955e−003
6	2.1172e+000	3.5905e−004
7	2.1131e+000	2.4352e−004
8	2.1080e+000	1.8644e−004
9	1.7357e+000	1.8016e−004
10	1.7043e+000	1.7929e−004
11	8.8174e−001	1.7868e−004
12	3.8732e−001	1.7743e−004

Table 2 Mean H^1 velocity relative errors for different $\varepsilon_{\max} = 10^{-3}$ and $\varepsilon_{\max} = 10^{-4}$, imposed on all $g^j_M(x, \mu)$ (considering several different μ test values)

N	$\varepsilon_{\max} = 10^{-3}$	$\varepsilon_{\max} = 10^{-4}$
1	4.2656e−001	4.2653e−001
2	1.3708e−001	1.3709e−001
3	2.1880e−002	2.1886e−002
4	1.5963e−002	1.5964e−002
5	4.9358e−003	4.9388e−003
6	1.9177e−004	1.9183e−004
7	6.7685e−005	6.7584e−005
8	8.2645e−006	8.1374e−006
9	1.9044e−006	1.7880e−006
10	9.0032e−007	7.7022e−007
11	1.5746e−007	2.6138e−008
12	1.5181e−007	1.8676e−008

Table 3 Mean H^1 velocity relative errors for different $\varepsilon_{\max} = 10^{-5}$, $\varepsilon_{\max} = 10^{-6}$ and comparison with true $g^j(\mu, x)$ functions (considering several different μ test values)

N	$\varepsilon_{\max} = 10^{-5}$	$\varepsilon_{\max} = 10^{-6}$	exact g^j
1	4.2654e−001	4.2654e−001	4.2654e−001
2	1.3709e−001	1.3709e−001	1.3709e−001
3	2.1885e−002	2.1884e−002	2.1884e−002
4	1.5963e−002	1.5963e−002	1.5963e−002
5	4.9380e−003	4.9380e−003	4.9380e−003
6	1.9180e−004	1.9181e−004	1.9181e−004
7	6.7581e−005	6.7582e−005	6.7582e−005
8	8.1348e−006	8.1356e−006	8.1356e−006
9	1.7812e−006	1.7813e−006	1.7813e−006
10	7.6544e−007	7.6542e−007	7.6542e−007
11	2.2070e−008	2.1981e−008	2.1980e−008
12	1.4503e−008	1.4421e−008	1.4421e−008

$$\nu_T = \nu \begin{bmatrix} \sum_{m=1}^{M^a_{11}} \beta_{11m}(\mu) \gamma_{11m}(x) & \sum_{m=1}^{M^a_{12}} \beta_{12m}(\mu) \gamma_{12m}(x) \\ \sum_{m=1}^{M^a_{21}} \beta_{21m}(\mu) \gamma_{21m}(x) & \sum_{m=1}^{M^a_{22}} \beta_{22m}(\mu) \gamma_{22m}(x) \end{bmatrix}.$$

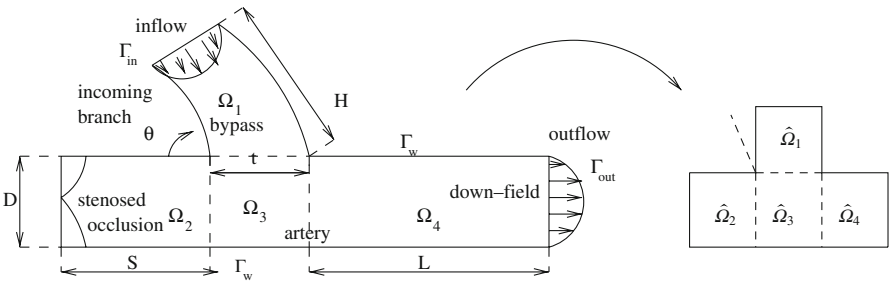

Fig. 5 Geometrical scheme for the bypass test problem (physical domain and reference one)

Note that this tensor is symmetric. Moreover,

$$\chi_T = \begin{bmatrix} \sum_{m=1}^{M_{11}^b} \alpha_{11m}(\mu)\omega_{11m}(x) & \sum_{m=1}^{M_{12}^b} \alpha_{12m}(\mu)\omega_{12m}(x) \\ 0 & 1 \end{bmatrix}.$$

The index r referring to every different subdomain is omitted.

– At this step, having defined all the abstract formulations of the previous sections, we have applied the reduced basis method and assembled the approximation spaces as described in Sect. 4.
– Tables 1, 2 and 3 show numerical results (mean H^1 relative errors on velocity, testing a large number of configurations for very different μ) at different N and different max interpolation error $\varepsilon_{\max}$. At the end of the test we have carried out a comparison between empirical interpolation (applied to $g_M^j(x,\mu)$ terms) and "true" functions ($g^j(x,\mu)$). We can see that for $\varepsilon_{\max} \leq 10^{-4}$ we have a good convergence (typical of reduced basis method, see [14]) and results are not dominated or influenced by interpolation error. When the interpolation error is dominating the reduced basis error is characterized by a constant "plateau" and is not diminished by increasing N (see for example the case in which $\varepsilon_{\max} \geq 10^{-2}$ of Table 1). It may happen that increasing N further the plateau is diminishing very slowly, but the method would not be efficient and the dimension of N would be too big. Another aspect is related with the number of function $M_{\max}$ used to interpolate $g^j(x,\mu)$: having different $g_M^j(x,\mu)$ function we have reported results as function of the maximum interpolation error allowed. In any case for the most complex function to be interpolated and for the lowest interpolation error fixed the value of $M_{\max}$ is always less or equal to the value of N considered and so $O(10)$. The scope of this paper is to demonstrate reduced basis method properties in presence of non-affine parametric dependence at the minimum $M_{\max}$ possible, to contain also the computational costs for interpolation procedure. Concerning computational costs, once we have set all the off-line calculation (performed only once to build reduced basis approximation spaces and done on the reference domain), the on-line costs are very low. For example, considering Table 3, the computational cost for each on-line calculation (with a different value of the parameter μ and a basis built with $N = 12$) is 12% if compared with the cpu time used to compute one finite element solution. The accuracy reached is of order 10^{-8}. These computational costs agree with the ones reported in [30].

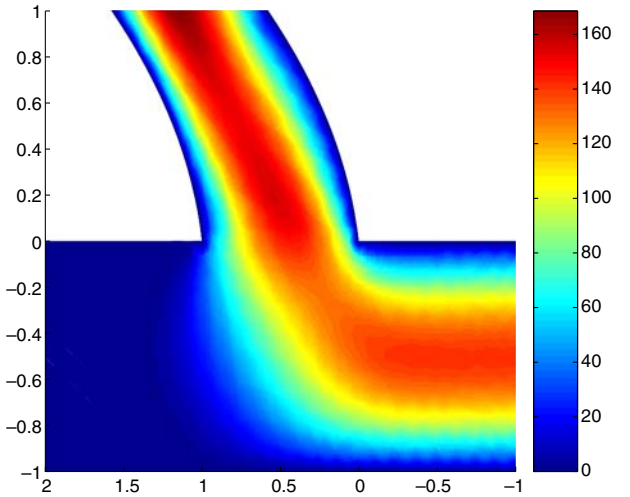

Fig. 6 Haemodynamic flow (velocity absolute value) in bypass subject to curved wall and graft angle ($\upsilon = 0.41$ and $\theta = \pi/3$)

5.2 Second test: bypass with curved incoming branch

We introduce a vector of parameters $\mu = \{t, D, L, S, H, \theta, \upsilon\} \in \mathcal{D}^\mu \subset \mathbb{R}^P$, $\mathcal{D}^\mu$ is given by: $[t_{\min}, t_{\max}] \times [D_{\min}, D_{\max}] \times [L_{\min}, L_{\max}] \times [S_{\min}, S_{\max}] \times [H_{\min}, H_{\max}] \times [\theta_{\min}, \theta_{\max}] \times [\upsilon_{\min}, \upsilon_{\max}]$. For a schematic view of the problem see Fig. 5. In this problem we have affine and non-affine parameter dependence in different subdomains. The aim of the test is to combine the study of affine and the non-affine terms in the same problem by varying different geometrical parameters and then to

Table 4 H^1 velocity relative errors for $\varepsilon_{\max} = 10^{-5}$: (a) only υ (non-affine) parameter varying

N	H^1 mean (a)	H^1 max (a)
1	4.8058e−02	1.3605e−01
2	1.5528e−03	2.3202e−03
3	7.1431e−06	1.0378e−05
4	1.6258e−07	8.2429e−07
5	6.1010e−10	1.4106e−09
6	7.0100e−12	3.2120e−11

Table 5 L^2 pressure relative errors for $\varepsilon_{\max} = 10^{-5}$: (a) only υ (non-affine) parameter varying

N	L^2 mean (a)	L^2 max (a)
1	1.3110e−03	3.3078e−03
2	4.8437e−05	7.2138e−05
3	2.0062e−07	3.0323e−07
4	2.0674e−09	1.0903e−08
5	8.9100e−12	2.1080e−11
6	1.1200e−13	5.3320e−13

test reduced basis convergence. Referring to notation in Sect. 3 we have $R_G = 3$ (number of subdomains with affine dependence, i.e. $\Omega_2, \Omega_3, \Omega_4$), $R_T = 1$ (number of subdomains with non-affine dependence, i.e. Ω_1). For more information on this application dealing only with affine parameters dependence we suggest to see [32]. The coordinate transformation in Ω_1 with non-affine parameter dependence is given by

$$\begin{cases} x_1 = \frac{1}{H}\hat{x}_1 \\ x_2 = \frac{1}{t}(\hat{x}_2 - (\upsilon H^2 x_1(x_1 - 1) + H x_1 \tan(\theta))) \end{cases} \tag{22}$$

The role of parameters t and H is to stretch subdomain Ω_1 (as L, S, D stretch the remaining subdomains), the parameter υ introduces a curvature in the walls of the incoming branch of the bypass and θ is responsible for a rigid rotation varying the graft angle. The tensors for *bilinear forms* are given by:

$$\nu_T^1 = \nu \begin{bmatrix} \frac{t}{H} & -(\tan\theta + 2\upsilon H x_1 - \upsilon H) \\ -(\tan\theta + 2\upsilon H x_1 - \upsilon H) & \frac{(1+(\tan\theta+2\upsilon H x_1 - \upsilon H)^2)}{t} H \end{bmatrix}; \tag{23}$$

$$\nu_G^2 = \nu \begin{bmatrix} \frac{S}{D} & 0 \\ 0 & \frac{D}{S} \end{bmatrix}; \quad \nu_G^3 = \nu \begin{bmatrix} \frac{t}{D} & 0 \\ 0 & \frac{D}{t} \end{bmatrix}; \quad \nu_G^4 = \nu \begin{bmatrix} \frac{L}{D} & 0 \\ 0 & \frac{D}{L} \end{bmatrix}. \tag{24}$$

The tensors for *pressure and divergence linear forms* are given by:

$$\chi_T^1 = \begin{bmatrix} t & -H(\tan\theta + 2\upsilon H x_1 - \upsilon H) \\ 0 & H \end{bmatrix}; \tag{25}$$

$$\chi_G^2 = \begin{bmatrix} S & 0 \\ 0 & D \end{bmatrix}; \chi_G^3 = \begin{bmatrix} t & 0 \\ 0 & D \end{bmatrix}; \quad \chi_G^4 = \begin{bmatrix} L & 0 \\ 0 & D \end{bmatrix}. \tag{26}$$

We have applied empirical interpolation expansion to the components of tensor ν_T^1 and χ_T^1 and built reduced basis approximation.

We have carried out four different tests based on the same geometry but with different parameters:

Table 6 H^1 velocity relative errors for $\varepsilon_{\max} = 10^{-5}$: (b) υ, L, S (affine and non-affine) parameters (in different subdomains) varying

N	H^1 mean (b)	H^1 max (b)
1	6.63847e−02	1.01112e−01
2	3.94004e−02	9.82942e−02
3	3.46897e−03	4.68399e−03
4	3.16378e−03	3.65756e−03
5	8.58429e−04	2.31849e−03
6	1.29567e−04	2.72338e−04
7	5.51890e−05	4.23899e−05
8	3.18091e−05	3.83384e−05
9	1.23528e−05	2.26590e−05
10	7.29802e−06	9.86723e−06
11	1.51548e−06	2.30932e−06
12	2.34584e−07	5.31751e−07
13	1.21290e−07	2.40584e−07
14	7.51433e−08	1.18963e−07
15	3.23837e−08	9.11491e−08

Table 7 L^2 pressure relative errors for $\varepsilon_{\max} = 10^{-5}$: (b) υ, L, S (affine and non-affine) parameters (in different subdomains) varying

N	L^2 mean (b)	L^2 max (b)
1	4.97657e−02	7.64428e−02
2	1.44390e−03	2.40459e−03
3	2.18353e−04	2.23485e−03
4	1.17247e−04	1.54309e−04
5	2.26938e−05	5.85041e−05
6	2.98422e−06	7.29587e−06
7	9.68781e−07	2.04184e−06
8	4.43647e−07	5.17774e−07
9	1.55099e−07	2.51658e−07
10	7.90834e−08	1.29403e−07
11	1.86052e−08	2.98586e−08
13	2.30951e−09	6.43834e−09
14	1.5816e−09	2.43859e−09
15	6.0645e−10	1.32561e−09

(a) we consider only υ parameter to create a curvature in the wall, we deal only with non-affine mapping in one subdomain where we apply empirical interpolation;

Table 8 H^1 velocity relative errors for $\varepsilon_{\max} = 10^{-5}$: (c) υ, L, S, t parameters varying

N	H^1 mean (c)	H^1 max (c)
1	5.63465e−01	1.10659e+00
2	1.55181e−01	4.26078e−01
3	2.33882e−02	6.28938e−02
4	6.96864e−03	1.35431e−02
5	2.41075e−03	7.54956e−03
6	7.40550e−04	1.92401e−03
7	4.42849e−04	1.72777e−03
8	2.24509e−04	7.84976e−04
9	6.57733e−05	3.60971e−04
10	1.22527e−05	8.02970e−05
11	3.46346e−06	2.09716e−05
12	1.01101e−06	7.81558e−06
13	1.91343e−07	1.04166e−06
14	2.38061e−08	2.38061e−07

Table 9 L^2 pressure relative errors for $\varepsilon_{\max} = 10^{-5}$: (c) υ, L, S, t parameters varying

N	L^2 mean (c)	L^2 max (c)
1	3.95384e−01	7.10666e−01
2	6.90123e−03	1.32884e−02
3	4.13599e−03	8.82405e−03
4	9.17813e−04	2.12774e−03
5	2.17614e−04	7.09398e−04
6	1.02036e−05	4.78661e−04
7	4.40703e−05	1.89533e−04
8	2.55188e−05	1.05753e−04
9	4.03863e−06	2.22016e−05
10	5.14632e−07	3.87984e−06
11	3.35225e−07	2.72714e−06
12	3.06439e−07	2.68244e−06
13	2.11621e−08	1.12451e−07
14	3.04801e−09	3.04801e−08

(b) then, we consider υ and also parameters L and S, each of them is operating into different subdomains and we combine affine and non-affine transformations;

(c) in the third test we consider parameters υ, L, S and t so that we have more parameters in the same subdomain subject to non-affine parameter dependence;

(d) in the last term we introduce also graft angle θ so that we have rigid rotation, stretching (due to t or/and H) and curvature (due to υ) in the same subdomain. Figure 6 shows an example of haemodynamic flow in our curved geometry.

In Tables 4, 5, 6, 7, 8, 9, 10 and 11 we report numerical results (H^1 errors on velocity and L^2 errors on pressure for each test case) considering about 50 configurations at different N for different test cases (a)–(d). The maximum interpolation error considered has been

Table 10 H^1 velocity relative errors for $\varepsilon_{\max} = 10^{-5}$: (d) $\upsilon, t, L, S, \theta$ parameters varying

N	H^1 mean (d)	H^1 max (d)
1	4.87915e−01	3.90400e+00
2	3.02592e−01	1.38505e+00
3	2.43772e−01	5.11847e−01
4	3.28557e−02	6.75237e−02
5	1.82035e−02	4.82212e−02
6	9.24689e−03	3.51396e−02
7	7.74796e−03	2.29014e−02
8	2.55247e−03	1.26095e−02
9	1.33895e−03	1.25823e−02
10	5.34446e−04	1.97937e−03
11	3.21415e−04	1.39168e−03
12	2.07283e−04	9.36665e−04
13	1.23885e−04	9.30468e−04
14	8.34764e−05	3.40849e−04
15	3.74193e−05	2.60742e−04
16	1.41356e−05	8.64251e−05
17	8.12437e−06	4.87599e−05
18	5.44325e−06	3.61402e−05

Table 11 L^2 pressure relative errors for $\varepsilon_{\max} = 10^{-5}$: (d) $\upsilon, t, L, S, \theta$ parameters varying

N	L^2 mean (d)	L^2 max (d)
1	1.45944e−01	2.40938e−01
2	5.12837e−02	1.41755e−01
3	2.21637e−02	7.52749e−02
4	2.32357e−03	6.47304e−03
5	2.22706e−03	4.97473e−03
6	6.09347e−04	1.65196e−03
7	5.77145e−04	1.41329e−03
8	2.39322e−04	1.27309e−03
9	1.22951e−04	6.23509e−04
10	7.20850e−05	5.11114e−04
11	2.59278e−05	9.45923e−05
12	2.04926e−05	8.20901e−05
13	8.85109e−06	6.95491e−05
14	6.46217e−06	5.33563e−05
15	2.02932e−06	2.76802e−05
16	8.98324e−07	1.00723e−05
17	2.92535e−07	1.17173e−06
18	1.99739e−07	1.00675e−06

$\varepsilon_{\max} = 10^{-5}$ not to have interpolation error dominating our approximation and to avoid a constant "plateau" in error plots (thus affecting the efficiency of reduced basis method). Figure 7 shows as example the off-line set of parameters used in test case (d) (the most complex one) used to store the basis functions by the adaptively optimized assembling procedure we used, introduced in Sect. 4.1 and in [21,30]. Also in this second test case on-line computational costs for the maximum value of N shown in the errors tables are between 12 and 15% with respect to a finite element calculation.

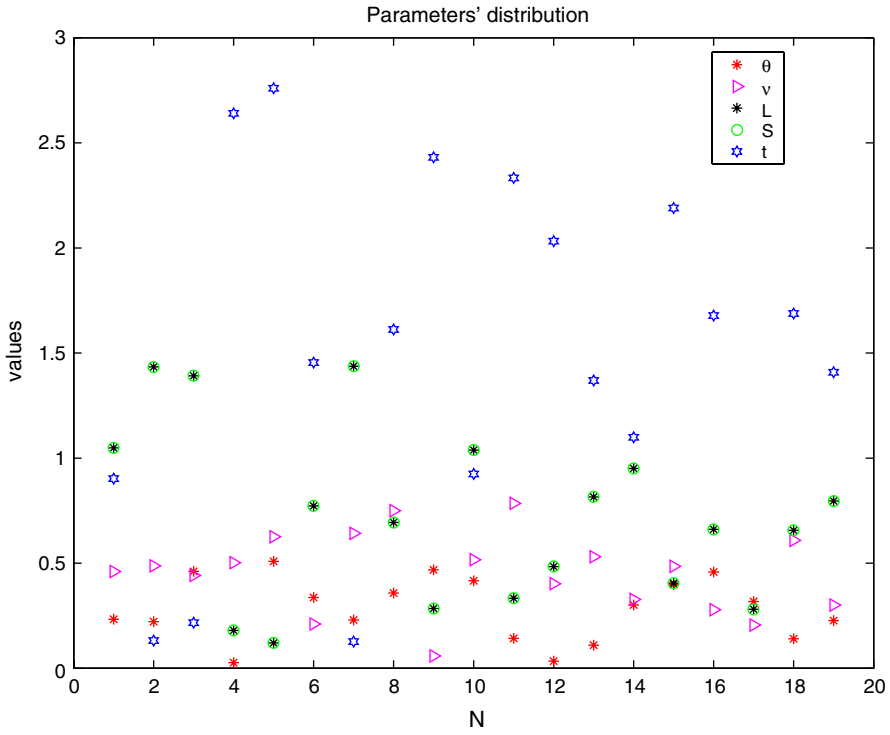

Fig. 7 Parameters distribution during off-line optimized basis assembling procedures [test case (d)]

6 Conclusions

In this paper the aim is to expand and apply efficient, accurate and real-time reduced basis techniques on biomechanics problems using realistic geometries such as biomedical devices optimization problem (for example a bypass). See [26] for a shape design problem combined with optimal control and [31] for a "multilevel" optimization approach. The goal is to combine reduced basis techniques with shape design and optimal control related problem such as [1], where shape optimization in reference domain and non-affine mapping have been considered. Results have shown that it is possible to consider more complex geometries in optimization problems using reduced basis techniques and introducing empirical interpolation for non-affine mapping terms preserving reduced basis methods properties, first of all rapid and accurate convergence.

Acknowledgements Acknowledgements to Prof. A.T. Patera of Massachusetts Institute of Technology, Prof. A. Quarteroni of EPFL and MOX-Politecnico di Milano, Prof. Y. Maday of University Paris VI, Dr. K. Veroy (MIT) and Dr. N.C. Nguyen (National University of Singapore, Singapore-MIT Alliance) for supervision, suggestions, very helpful discussions, comments and insights. G. Rozza acknowledges the support provided through the European Community's Human Potential Programme under contract HPRN-CT-2002-00270 HaeMOdel and Swiss National Science Foundation (PBEL2-111646).

References

1. Agoshkov, V., Quarteroni, A., Rozza, G.: Shape design in aorto-coronaric bypass using perturbation theory. SIAM J. Numer. Anal. **44**(1), 367–384 (2006)
2. Almroth, B.O., Stern, P., Brogan, F.A.: Automatic choice of global shape functions in structural analysis. AIAA J. **16**, 525–528 (1978)
3. Balmes, E.: Parametric families of reduced finite element models. Theory and applications. Mech. Syst. Signal. Process. **10**(4), 381–394 (1996)
4. Barrault, M., Maday, Y., Nguyen, N.C., Patera, A.T.: An "empirical interpolation" method: application to efficient reduced-basis discretization of partial differential equations. C. R Acad. Sci. Paris Anal. Numerique **339**, 667–672 (2004)
5. Barrett, A., Reddien, G.: On the reduced basis method. Z. Angew. Math. Mech. **75**(7), 543–549 (1995)
6. Fink, J.P., Rheinboldt, W.C.: On the error behavior of the reduced basis technique for non-linear finite element approximations. Z. Angew. Math. Mech. **63**(1), 21–28 (1983)
7. Galdi, G.P.: An Introduction to the Mathematical Theory of the Navier–Stokes Equations, Volume I: Linearized Steady Problem. Springer, Berlin Heidelberg New York (1994)
8. Girault, V., Raviart, P.A.: Finite Element Methods for Navier–Stokes Equations. Springer, Berlin Heidelberg New York (1986)
9. Gresho, P.M., Sani, R.L.: Incompressible Flow and the Finite Elements Method Wiley, New York (2000)
10. Gunzburger, M.D.: Finite Element Method for Viscous Incompressible Flows: A Guide to Theory, Practice, and Algorithms. Academic, Boston (1989)
11. Ito, K., Ravindran, S.S.: A reduced basis method for control problems governed by PDEs. In: Desch, W., Kappel, F., Kunish, K. (eds.) Control and Estimation of Distributed Parameter System, pp 153–168. Birkäuser, Basel (1998)

12. Ito, K., Ravindran, S.S.: A reduced-order method for simulation and control of fluid flow. J. Comput. Phys. **143**(2), 403–425 (1998)
13. Lions, P.L.: Mathematical Topics in Fluid Mechanics. Volume I: Incompressible Models. Oxford Science Publications, Clarendon Press, Oxford (1996)
14. Maday, Y., Patera, A.T., Turinici, G.: Global a priori convergence theory for reduced-basis approximations of single-parameter symmetric coercive elliptic partial differential equations. C. R. Acad. Sci. Paris Série I **335**, 1–6 (2002)
15. Maday, Y., Patera, A.T., Turinici, G.: A priori convergence theory for reduced-basis approximations of single-parameter elliptic partial differential equations. J. Sci. Comput. **17**(1), 437–446 (2002)
16. Nagy, D.A.: Modal representation of geometrically non-linear behaviour by the finite element method. Comput. Struct. **10**, 683–688 (1979)
17. Nguyen, N.C., Veroy, K., Patera, A.T.: Certified real-time solution of parametrized partial differential equations. In: Catlow, R., Shercliff, H., Yip, S. (eds.) Handbook of Materials Modeling. Springer, Berlin Heidelberg New York (2005)
18. Mohammadi, B., Pironneau, O.: Applied Shape Optimization for Fluids. Oxford University Press, Oxford (2001)
19. Peterson, J.S.: The reduced basis method for incompressible viscous flow calculations. SIAM J. Sci. Stat. Comput. **10**(4), 777–786 (1989)
20. Porsching, T.A.: Estimation of the error in the reduced basis method solution of non-linear equations. Math. Comput. **45**(172), 487–496 (1995)
21. Prud'homme, C.: Adaptive reduced basis space generation and approximation. (submitted) (2005)
22. Prud'homme, C., Rovas, D., Veroy, K., Maday, Y., Patera, A.T., Turinici, G.: Reliable real-time solution of parametrized partial differential equations: reduced-basis output bound methods. J. Fluids Eng. **172**, 70–80 (2002)
23. Prud'homme, C., Patera, A.T.: Reduced-basis output bounds for approximately parametrized elliptic coercive partial differential equations. Comput. Vis. Sci. **6**(2–3), 147–162 (2004)
24. Prud'homme, C., Rovas, D., Veroy, K., Patera, A.T.: Mathematical and computational framework for reliable real-time solution of parametrized partial differential equations. M2AN **36**(5), 747–771 (2002)
25. Quarteroni, A., Formaggia, L.: Mathematical modelling and numerical simulation of the cardiovascular system in modelling of living systems. In: Ciarlet, P.G., Lions, J.L. (eds.) Handbook of Numerical Analysis Series, vol. XII. Elsevier, Amsterdam (2004)
26. Quarteroni, A., Rozza, G.: Optimal control and shape optimization of aorto-coronaric bypass anastomoses. M^3AS **13**(12), 1801–1823 (2003)
27. Quarteroni, A., Valli, A.: Numerical Approximation of Partial Differential Equations. Springer, Berlin Heidelberg New York (1994)
28. Rheinboldt, W.C.: On the theory and error estimation of the reduced basis method for multi-parameter problems. Nonlinear Anal. Theory Methods Appl. **21**(11), 849–858 (1993)
29. Rovas, D.: Reduced-Basis Output Bound Methods for Parametrized Partial Differential Equations. PhD Thesis, MIT, Massachusetts Institute of Technology (2003)
30. Rozza, G., Veroy, K.: On the stability of the reduced basis method for Stokes equations in parametrized domains. Comput. Methods Appl. Mech. Eng. (in press) (2006)
31. Rozza, G.: On optimization, control and shape design of an arterial bypass. Int. J. Numer. Methods Fluids **47**(10–11), 1411–1419 (2005)
32. Rozza, G.: Real time reduced basis techniques in arterial bypass geometries. In: Bathe, K.J. (ed.) Computational Fluid Dynamics and Solid Mechanics, pp 1284–1288. Elsevier, Amsterdam (2005)
33. Solodukhov, Y.: Reduced-Basis Methods Applied to Locally Non-Affine Problems. PhD Thesis, MIT, Massachusetts Institute of Technology (2004)
34. Taylor, C., Hood, P.: A numerical solution of the Navier–Stokes equations using the finite element technique. Comput. Fluids **1**, 73–100 (1973)
35. Veroy, K., Patera, A.T.: Certified real-time solution of the parametrized steady incompressible Navier–Stokes equations; rigorous reduced-basis a posteriori error bounds. Int. J. Numer. Methods Fluids **47**(8–9), 773–788 (2005)
36. Veroy, K., Patera, A.T.: Reduced-basis approximation of the viscosity-parametrized incompressible Navier–Stokes equation: rigorous a posteriori error bounds. Proceedings of Singapore-MIT Alliance Symposium, January (2004)
37. Veroy, K.: Reduced-Basis Methods Applied to Problems in Elasticity. PhD Thesis, MIT, Massachusetts Institute of Technology (2003)